RESEARCH

Time-Continuous and Time-Discrete SIR Models Revisited: Theory and Applications

Benjamin Wacker[1*] and Jan Schlüter[1,2]

*Correspondence: bewa87@gmx.de
[1]Next Generation Mobility Group, Max-Planck-Institute for Dynamics and Self-Organization, Department of Dynamics of Complex Fluids, Am Fassberg 17, D-37077 Göttingen, Germany
Full list of author information is available at the end of the article

Abstract

Since Kermack and McKendrick have introduced their famous epidemiological SIR model in 1927, mathematical epidemiology has grown as an interdisciplinary research discipline including knowledge from biology, computer science or mathematics. Due to current threatening epidemics, this interest is continuously rising. As our main goal, we establish an implicit time-discrete SIR (susceptible people - infectious people - recovered people) model. Fur this purpose, we first introduce its continuous variant with a time-varying transmission rate and, as our first contribution, discuss thoroughly its properties. With respect to these results, we develop different possible time-discrete SIR models, we derive our implicit time-discrete SIR model in contrast to many other works regarding mainly explicit time-discrete schemes and, as our main contribution, show unique solvability and further desirable properties compared to its continuous version. We thoroughly show that many of the desired properties of the time-continuous case are still valid in the time-discrete implicit case. Finally, we apply our proposed time-discrete SIR model to currently available data regarding the spread of COVID-19 in France and Iran.

Keywords: COVID-19; Difference Equations; Existence and Uniqueness; Mathematical Epidemiology; Non-Linear Ordinary Differential Equations; SIR Model

1 Introduction

Since its outbreak in Wuhan (China) in December 2019, the pandemic outbreak of COVID-19 threatens people worldwide. Politicians around the globe have to balance different interests and need to make tremendous decisions which impact our daily life. For these reasons, governments around the world heavily rely on scientific advices in the present situation. Thus, John Hopkins University collects epidemiological data regarding COVID-19 from many countries during the last months [1, 2]. Additionally, many biological and medical studies regarding different aspects of this new corona-virus have been rapidly appeared in scientific journals [3, 4, 5, 6, 7, 8, 9]. However, to estimate the impact of COVID-19, governments need forecasts from as many models as possible.

Kermack and McKendrick introduced the now well-known SIR model in one of mathematical epidemiology's most groundbreaking work in 1927 [10]. They assumed a fixed population size and divided this population into three different homogeneous groups of people, namely susceptible people, infectious people and recovered people - excluding births, deaths and deaths by disease from their model. Due to its success and simplicity, their works were reprinted in 1991 [11, 12, 13]. In upcoming decades, epidemiologists and mathematicians have developed many variants and extensions of this basic model by, for example, adding age or spatial structures [14, 15, 16, 17, 18].

After the outbreak of COVID-19, many scientists are recently publishing articles with emphasis on epidemic forecasts which strongly relate to mathematical models. Many approaches, mainly focusing on stochastic arguments, with respect to predicting forecasts of the total number of infected people have been appeared during the last weeks [19, 20, 21, 22, 23, 24] or in the past [25, 26]. Recently, neural networks have been applied to forecasting [27].

There are many works with respect to SIR models [28, 29] and its time-discrete versions [30, 31, 32, 33]. However, one find mainly explicit schemes with respect to time-discrete SIR models in the aforementioned works and references therein. For this reason, we summarize and extend some results on properties of the time-continuous classical SIR model and, as our main contribution, we propose an implicit time-discrete version of this classical SIR model and prove that this time-discrete variant maintains many of time-continuous version's properties. Subsequently, we briefly describe the numerical algorithm and apply it to three current scenarios of the spread of COVID-19 in France and Iran. In conclusion, we state our main results and shortly give an outlook of possible future research.

2 Time-Continuous SIR Model

In this section, we portray the time-continuous SIR model and its properties.

2.1 Mathematical Background Material

Here, we recall Lipschitz continuity of a function on Euclidean spaces.

Definition 1 ([34, Subsection 3.2]) *Let $d_1, d_2 \in \mathbb{N}$. If $S \subset \mathbb{R}^{d_1}$, a defined function $\mathbf{F}\colon S \longrightarrow \mathbb{R}^{d_2}$ is called* Lipschitz continuous on S *if there exists a non-negative constant $L \geq 0$ such that*

$$\left\| \mathbf{F}\left(\mathbf{x}\right) - \mathbf{F}\left(\mathbf{y}\right) \right\|_{\mathbb{R}^{d_2}} \leq L \cdot \left\| \mathbf{x} - \mathbf{y} \right\|_{\mathbb{R}^{d_1}} \tag{1}$$

holds for all $\mathbf{x}, \mathbf{y} \in S$. Here, $\|\cdot\|$ denotes a suitable norm on the corresponding Euclidean space.

Let $U \subset \mathbb{R}^{d_1}$ be open, let $\mathbf{F}\colon U \longrightarrow \mathbb{R}^{d_2}$. We shall call $\mathbf{F}$ locally Lipschitz continuous *if for every point $\mathbf{x_0} \in U$ there exists a neighborhood V of $\mathbf{x_0}$ such that the restriction of $\mathbf{F}$ to V is Lipschitz continuous on V.*

In a more general framework, we consider a non-linear initial value problem

$$\begin{cases} \mathbf{z}'(t) = \mathbf{G}(t, \mathbf{z}(t)), \\ \mathbf{z}(0) = \mathbf{z_0} \end{cases} \tag{2}$$

where we define our solution vector $\mathbf{z}(t) = (x_1(t), \ldots, x_n(t))$, our vectorial function $\mathbf{G}(t, \mathbf{z}(t)) = (g_1(t, \mathbf{z}(t)), \ldots, g_n(t, \mathbf{z}(t)))$ and our initial condition $\mathbf{z_0} \in \mathbb{R}^n$. To conclude global existence and uniqueness, we can apply the following theorem that is a direct consequence of Grönwall's lemma.

Theorem 1 ([34, Theorem 4.2.1]) *If $\mathbf{F}\colon \mathbb{R}^n \longrightarrow \mathbb{R}^n$ is locally Lipschitz continuous and if there exist non-negative real constants B and K such that*

$$\|\mathbf{G}(t, \mathbf{z}(t))\|_{\mathbb{R}^n} \leq K \cdot \|\mathbf{z}(t)\|_{\mathbb{R}^n} + B \tag{3}$$

holds for all $\mathbf{z}(t) \in \mathbb{R}^n$, then the solution of the initial value problem (2) exists for all time $t \in \mathbb{R}$ and moreover, it holds

$$\|\mathbf{z}(t)\|_{\mathbb{R}^n} \leq \|\mathbf{z_0}\|_{\mathbb{R}^n} \cdot \exp(K \cdot |t|) + \frac{B}{K} \cdot (\exp(K \cdot |t|) - 1) \tag{4}$$

for all $t \in \mathbb{R}$.

2.2 Continuous Problem Formulation

At first, let us state the model's assumptions [16, 17]:

1) The population's size N is fixed over time, i.e. $N(t) = N$ for all $t \in [0, \infty)$;
2) We divide a population into three homogeneous subgroups, namely susceptible people (S), infectious people (I) and recovered people (R). We can clearly

assign every individual to exactly one subgroup. Hence, we obtain

$$N = S\left(t\right) + I\left(t\right) + R\left(t\right) \tag{5}$$

for all $t \in [0, \infty)$;

3) Additionally, no births and deaths occur;

4) The time-varying transmission rate $\alpha\colon [0, \infty) \longrightarrow [0, 1]$ is Lipschitz continuous, continuously differentiable and it holds $\lim\limits_{t \to \infty} \alpha\left(t\right) = 0$;

5) The recovery rate $\beta \in [0, 1]$ is constant in time.

Furthermore, we exclude age structures or spatial relationships from our time-continuous model [16, 18]. For abbreviation, we write $f'\left(t\right) := \dfrac{\mathrm{d}f\left(t\right)}{\mathrm{d}t}$. Our equations of the time-continuous SIR model read

$$\begin{cases} S'\left(t\right) = -\alpha\left(t\right) \cdot \dfrac{I\left(t\right) \cdot S\left(t\right)}{N}, \\ I'\left(t\right) = \alpha\left(t\right) \cdot \dfrac{S\left(t\right) \cdot I\left(t\right)}{N} - \beta \cdot I\left(t\right), \\ R'\left(t\right) = \beta \cdot I\left(t\right) \end{cases} \tag{6}$$

with initial conditions $S\left(0\right) = S_1 > 0$, $I\left(0\right) = I_1 > 0$ and $R\left(0\right) = R_1 \geq 0$. We portray a chart of the flow between the different three subgroups in Figure 1. Obviously, the equation

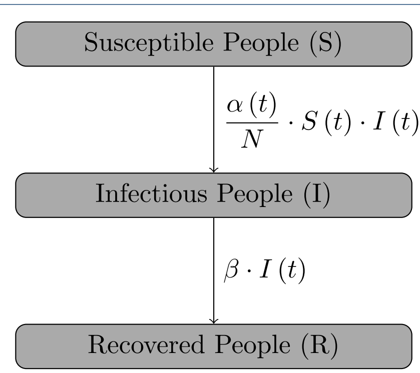

Figure 1 Flowchart of the three different subgroups described by the time-continuous SIR model

$$N'(t) = S'(t) + I'(t) + R'(t) = 0$$

is valid and hence, the first assumption is fulfilled.

2.3 Global Existence and Uniqueness

In contrast to many other works, we formulate a theorem regarding global existence and uniqueness of (6) based on Theorem 1.

Theorem 2 *The non-linear first order ordinary differential equation system (6) has a unique solution which exists for all $t \geq 0$.*

Proof By defining $\mathbf{z}(t) = (S(t), I(t), R(t))$, we can set

$$G\colon\ [0,\infty) \times \mathbb{R}^3 \longrightarrow \mathbb{R}^3\ ,\ \ (t, \mathbf{z}(t)) \longrightarrow \begin{pmatrix} -\alpha(t) \cdot \dfrac{I(t) \cdot S(t)}{N} \\ \alpha(t) \cdot \dfrac{S(t) \cdot I(t)}{N} - \beta \cdot I(t) \\ \beta \cdot I(t) \end{pmatrix}. \tag{7}$$

Clearly, G is Lipschitz continuous. By considering the maximum norm on our Euclidean space and applying the triangle inequality, we get

$$\begin{aligned} \|G(t, \mathbf{z}(t))\|_\infty &= \max\left\{\left|-\alpha(t)\,\frac{I(t) \cdot S(t)}{N}\right|, \left|\alpha(t)\,\frac{S(t) \cdot I(t)}{N} - \beta I(t)\right|, |\beta I(t)|\right\} \\ &\leq \max\left\{\left|\frac{I(t) \cdot S(t)}{N}\right|, \left|\frac{I(t) \cdot S(t)}{N}\right| + |I(t)|, |I(t)|\right\} \\ &\leq \|\mathbf{z}(t)\|_\infty \end{aligned}$$

from (7). Thus, all our assumptions of Theorem 1 are fulfilled and our proof is complete. $\square$

2.4 Solution's Boundedness

Now, we prove boundedness of the solution. For this purpose, we modify ideas from [17] and [35] because we, in contrast to them, consider a time-varying transmission rate $\alpha\colon\ [0,\infty) \longrightarrow [0,1]$.

Lemma 1 *Each solution function of (6) is bounded below by zero.*

Proof Here, we split the proof into three parts.

1) We first consider $S'(t) = -\alpha(t) \cdot \frac{I(t) \cdot S(t)}{N}$. Separation of variables leads to

$$\frac{S'(t)}{S(t)} = -\alpha(t) \cdot \frac{I(t)}{N}.$$

Integration yields

$$\ln\left(\frac{S(t)}{S_1}\right) = -\int_0^t \alpha(\tau) \cdot \frac{I(\tau)}{N}\,\mathrm{d}\tau$$

and this implies

$$S(t) = S_1 \cdot \exp\left(-\int_0^t \alpha(\tau) \cdot \frac{I(\tau)}{N}\,\mathrm{d}\tau\right)$$

Hence, it holds $S(t) > 0$ for all $t \geq 0$.

2) Let us continue with $I'(t) = \alpha(t) \cdot \frac{I(t) \cdot S(t)}{N} - \beta \cdot I(t)$. Separation of variables gives us

$$\frac{I'(t)}{I(t)} = \left(\alpha(t) \cdot \frac{S(t)}{N} - \beta\right)$$

and, applying the same argument as in our first step, we conclude

$$I(t) = I_1 \cdot \exp\left(\int_0^t \left\{\alpha(\tau) \cdot \frac{S(\tau)}{N} - \beta\right\} \mathrm{d}\tau\right).$$

This yields $I(t) > 0$ for all $t \geq 0$.

3) Finally, since $R'(t) = \beta \cdot I(t)$ holds, we clearly obtain

$$R(t) = R_1 + \beta \cdot \int_0^t I(\tau)\, \mathrm{d}\tau$$

and $R(t) \geq 0$ for all $t \geq 0$ is valid.

This completes our proof. □

Since $N = S(t) + I(t) + R(t)$ holds by our first assumption, we can finally state our boundedness theorem.

Theorem 3 *For all solution functions of* (6)*, we have:*

1) $0 \leq S(t) \leq N$*;*

2) $0 \leq I(t) \leq N$*;*

3) $0 \leq R(t) \leq N$

for all $t \geq 0$*.*

2.5 Further Properties

To conclude this section, we first investigate the solution's long-time behavior and summarize our results in the following theorem.

Theorem 4 *We get:*

1) S is monotonically decreasing and there exists a number $S^\star \geq 0$ *such that*

$$\lim_{t\to\infty} S(t) = S^\star;$$

2) R is monotonically increasing and there exists a number $R^\star \geq 0$ *such that*

$$\lim_{t\to\infty} R(t) = R^\star;$$

3) I is Lebesgue-integrable on $[0,\infty)$ and $\lim_{t\to\infty} I(t) = 0$

for all solution functions of (6).

Proof 1) Since $S'(t) \leq 0$ for all $t \geq 0$ and $0 \leq S(t) \leq S_0$ by Theorem 3, $S\colon [0,\infty) \longrightarrow [0,\infty)$ is monotonically decreasing and bounded below by zero. This implies the existence of $S^\star \geq 0$ such that $\lim_{t\to\infty} S(t) = S^\star$.

2) Since $R'(t) \geq 0$ for all $t \geq 0$ and $0 \leq R(t) \leq N$ is true by application of Theorem 3, $R\colon [0,\infty) \longrightarrow [0,\infty)$ is monotonically increasing and bounded above by N. This yields the existence of $R^\star \geq 0$ such that $\lim_{t\to\infty} R(t) = R^\star$.

3) Since $S'(t) = -\alpha(t) \cdot \dfrac{I(t) \cdot S(t)}{N}$ holds, integration yields

$$S_1 - S^\star = \int_0^\infty \frac{\alpha(\tau)}{N} \cdot S(\tau) \cdot I(\tau)$$

and because all functions $\alpha, S, I\colon [0,\infty) \longrightarrow [0,\infty)$ are non-negative, we obtain that I is Lebesgue-integrable on $[0,\infty)$ and $\lim_{t\to\infty} I(t) = 0$.

This finishes our proof. □

3 Time-Discrete Implicit SIR Model

In this section, we examine time-discrete versions of the given time-continuous SIR model (6). Let us assume that our time interval $[0,T]$ can be divided by a strictly increasing sequence $\{t_j\}_{j=1}^M$ for $M \in \mathbb{N}$ with $t_1 = 0$ and $t_M = T$. For abbreviation, we write $f(t_j) := f_j$ for all $j \in \{1,\ldots,M\}$.

3.1 Discussion of Formulations

Here, we only state a fully explicit scheme

$$\begin{cases} \dfrac{S_{j+1}-S_j}{t_{j+1}-t_j} = -\alpha_{j+1}\cdot\dfrac{I_j\cdot S_j}{N}, \\ \dfrac{I_{j+1}-I_j}{t_{j+1}-t_j} = \alpha_{j+1}\cdot\dfrac{I_j\cdot S_j}{N} - \beta I_j, \\ \dfrac{R_{j+1}-R_j}{t_{j+1}-t_j} = \beta I_j \end{cases} \tag{8}$$

and a fully implicit scheme

$$\begin{cases} \dfrac{S_{j+1}-S_j}{t_{j+1}-t_j} = -\alpha_{j+1}\cdot\dfrac{I_{j+1}\cdot S_{j+1}}{N}, \\ \dfrac{I_{j+1}-I_j}{t_{j+1}-t_j} = \alpha_{j+1}\cdot\dfrac{I_{j+1}\cdot S_{j+1}}{N} - \beta I_{j+1}, \\ \dfrac{R_{j+1}-R_j}{t_{j+1}-t_j} = \beta I_{j+1} \end{cases} \tag{9}$$

of the time-continuous SIR model (6) for all $j\in\{1,\dots,M-1\}$. Both formulations fulfill

$$N = S_{j+1}+I_{j+1}+R_{j+1} = S_j+I_j+R_j \tag{10}$$

for all $j\in\{1,\dots,M-1\}$. However, the fully explicit scheme (8) simply reduces to a linear system, while the fully implicit scheme (9) maintains the non-linear structure of the continuous problem formulation (6). For this reason, we investigate this fully implicit scheme in the following.

3.2 Time-Discrete Implicit Problem Formulation

We assume that $0\le a_j\le 1$ is given for all $j\in\{1,\dots,M\}$, that $0<\beta\le 1$ is valid, that $0<t_{j+1}-t_j\le 1$ for all $j\in\{1,\dots,M-1\}$ and that $S_1>0$, $I_1>0$ and

$R_1 \geq 0$ are given. An implicit solution scheme of (9) reads

$$\begin{cases} S_{j+1} = \dfrac{S_j}{1 + \alpha_{j+1} \cdot (t_{j+1} - t_j) \cdot \dfrac{I_{j+1}}{N}}, \\ I_{j+1} = \dfrac{I_j}{1 + \beta \cdot (t_{j+1} - t_j) - \alpha_{j+1} \cdot (t_{j+1} - t_j) \cdot \dfrac{S_{j+1}}{N}}, \\ R_{j+1} = R_j + \beta \cdot (t_{j+1} - t_j) \cdot I_{j+1} \end{cases} \tag{11}$$

for all $j \in \{1, \ldots, M-1\}$. Now, we are able to obtain an explicit solution scheme from (11) which even implies unique solvability for all $j \in \{1, \ldots, M-1\}$.

3.3 Unique Solvability

Our main ingredient is the equation

$$I_{j+1} = \frac{I_j}{1 + \beta \cdot (t_{j+1} - t_j) - \alpha_{j+1} \cdot (t_{j+1} - t_j) \cdot \dfrac{S_{j+1}}{N}} \tag{12}$$

from (11). Plugging

$$S_{j+1} = \frac{S_j}{1 + \alpha_{j+1} \cdot (t_{j+1} - t_j) \cdot \dfrac{I_{j+1}}{N}}$$

into (12) and writing $\Delta_{j+1} = (t_{j+1} - t_j)$ yields

$$I_{j+1} = \frac{(N + \alpha_{j+1} \cdot \Delta_{j+1} \cdot I_{j+1}) \cdot I_j}{(1 + \beta \cdot \Delta_{j+1}) \cdot (N + \alpha_{j+1} \cdot \Delta_{j+1} \cdot I_{j+1}) - \alpha_{j+1} \cdot \Delta_{j+1} \cdot S_j} \tag{13}$$

for all $j \in \{1, \ldots, M-1\}$. Hence, we get

$$\begin{aligned} &(1 + \beta \cdot \Delta_{j+1}) \cdot (\alpha_{j+1} \cdot \Delta_{j+1}) \cdot I_{j+1}^2 + (1 + \beta \cdot \Delta_{j+1}) \cdot N \cdot I_{j+1} \\ &= \alpha_{j+1} \cdot \Delta_{j+1} \cdot (S_j + I_j) \cdot I_{j+1} + N \cdot I_j \end{aligned}$$

and by setting

$$A := (1 + \beta \cdot \Delta_{j+1}) \cdot (\alpha_{j+1} \cdot \Delta_{j+1}) \tag{14}$$

and

$$B := \frac{(1 + \beta \cdot \Delta_{j+1}) \cdot N - \alpha_{j+1} \cdot \Delta_{j+1} \cdot (S_j + I_j)}{2}, \tag{15}$$

we get $A \cdot I_{j+1}^2 + 2 \cdot B \cdot I_{j+1} = N \cdot I_j$ and can finally conclude

$$I_{j+1} = -\frac{B}{A} + \sqrt{\frac{B^2}{A^2} + \frac{N \cdot I_j}{A}} \tag{16}$$

for all $j \in \{1, \ldots, M-1\}$. We now have an explicit solution formula for I_{j+1} for all $j \in \{1, \ldots, M-1\}$ and therefore also for S_{j+1} and R_{j+1} for all $j \in \{1, \ldots, M-1\}$. Summarizing our results, we can formulate the following theorem.

Theorem 5 *The implicit solution scheme* (11)

$$\begin{cases} S_{j+1} = \dfrac{S_j}{1 + \alpha_{j+1} \cdot (t_{j+1} - t_j) \cdot \dfrac{I_{j+1}}{N}}, \\ I_{j+1} = \dfrac{I_j}{1 + \beta \cdot (t_{j+1} - t_j) - \alpha_{j+1} \cdot (t_{j+1} - t_j) \cdot \dfrac{S_{j+1}}{N}}, \\ R_{j+1} = R_j + \beta \cdot (t_{j+1} - t_j) \cdot I_{j+1} \end{cases}$$

is uniquely solvable for all $j \in \{1, \ldots, M-1\}$. *It holds* (16)

$$I_{j+1} = -\frac{B}{A} + \sqrt{\frac{B^2}{A^2} + \frac{N \cdot I_j}{A}}$$

for all $j \in \{1, \ldots, M-1\}$ *with*

$$A := (1 + \beta \cdot \Delta_{j+1}) \cdot (\alpha_{j+1} \cdot \Delta_{j+1})$$

and

$$B := \frac{(1 + \beta \cdot \Delta_{j+1}) \cdot N - \alpha_{j+1} \cdot \Delta_{j+1} \cdot (S_j + I_j)}{2},$$

from (14) *and* (15)*.*

3.4 Additional Properties

We show that many of the continuous properties from Theorem 3 and Theorem 4 even translate to the time-discrete implicit scheme (11).

Theorem 6 *For our time-discrete implicit solution scheme* (11)*, we have:*

1) $0 \leq I_j \leq N$ *for all* $j \in \{1, \ldots, M\}$*;*

2) $0 \leq S_j \leq N$ *for all* $j \in \{1, \ldots, M\}$ *and* $S_{j+1} \leq S_j$ *for all* $j \in \{1, \ldots, M-1\}$*;*

3) $0 \leq R_j \leq N$ *for all* $j \in \{1, \ldots, M\}$ *and* $R_{j+1} \geq R_j$ *for all* $j \in \{1, \ldots, M-1\}$*;*

4) $\lim_{j \to \infty} I_j = 0$.

Proof 1) It holds $I_j \geq 0$ due to (16) and $I_j \leq N$ due to (10) for all $j \in \{1, \ldots, M\}$.

2) By our first properties and due to (10), we have the inequality $0 \leq S_j \leq N$ for all $j \in \{1, \ldots, M\}$. Again by our first property, we obtain

$$S_{j+1} = \frac{S_j}{1 + \alpha_{j+1} \cdot \Delta_{j+1} \cdot \dfrac{I_{j+1}}{N}} \leq S_j$$

for all $j \in \{1, \ldots, M-1\}$.

3) By our first property and due to (10), we get the inequality $0 \leq R_j \leq N$ for all $j \in \{1, \ldots, M\}$. Again by our first property, we conclude

$$R_{j+1} = R_j + \beta \cdot \Delta_{j+1} \cdot I_{j+1} \geq R_j$$

for all $j \in \{1, \ldots, M-1\}$.

4) Since $\lim\limits_{j \to \infty} \alpha_j = 0$ by assumption, there exists a $j^\star \in \mathbb{N}$ such that

$$\left| -\alpha_{j+1} \cdot \Delta_{j+1} \cdot \frac{S_{j+1}}{N} \right| \leq \frac{\beta}{2} \cdot \Delta_{j+1}$$

holds for all $j \geq j^\star$. This implies

$$I_{j+1} = \frac{I_j}{1 + \beta \cdot \Delta_{j+1} - \alpha_{j+1} \cdot \Delta_{j+1} \cdot \frac{S_{j+1}}{N}} \leq \frac{I_j}{1 + \frac{\beta}{2} \cdot \Delta_{j+1}}$$

for all $j \geq j^\star$. This finally yields $\lim\limits_{j \to \infty} I_j = 0$ by induction.

This completes our proof. □

3.5 Numerical Algorithm

We are now able to give a brief description of our numerical algorithm to solve the time-discrete implicit solution scheme (11). Here, we summarize our inputs, our computational steps and our algorithmic outputs. We sketch the resulting algorithm in Table 1.

Inputs:	- Initial values $S_1 > 0$, $I_1 > 0$ and $R_1 \geq 0$ - Time-varying transmission rate sequence $\{\alpha_j\}_{j=1}^M$ - Constant recovery rate β - Strictly increasing sequence $\{t_j\}_{j=1}^M$ of time points
Step 1:	- Compute all $\Delta_{j+1} = t_{j+1} - t_j$ for all $j \in \{1, \ldots, M-1\}$
Step 2:	- Compute I_{j+1} by (16), (15) and (14) for all $j \in \{1, \ldots, M-1\}$ - Compute S_{j+1} and R_{j+1} by (11) for all $j \in \{1, \ldots, M-1\}$
Outputs:	- Sequences $\{S_j\}_{j=1}^M$, $\{I_j\}_{j=1}^M$ and $\{R_j\}_{j=1}^M$

Table 1 Numerical algorithm for the time-discrete implicit SIR solution scheme (11)

4 Numerical Examples

We apply our time-discrete implicit SIR solution scheme (16) from Table 1 to available data regarding the spread of COVID-19 in France and Iran from John Hopkins University [1, 2]. The time period ranges from March 01, 2020 ($t_1 = 1$) to Mai 08, 2020 ($t_M = 69$). It holds $\Delta_{j+1} = t_{j+1} - t_j = 1$ for all $j \in \{1, \dots, M-1\}$.

4.1 Data Preprocessing

To apply our model, we have to process the given data of cumulative confirmed infected people $\left\{\widetilde{I}_j\right\}_{j=1}^{M}$, cumulative confirmed dead people $\left\{\widetilde{D}_j\right\}_{j=1}^{M}$ and cumulative confirmed recovered people $\left\{\widetilde{R}_j\right\}_{j=1}^{M}$. For our model, we need to compute

$$R_j = \widetilde{R}_j + \widetilde{D}_j, \qquad I_j = \widetilde{I}_j - R_j, \qquad S_j = N - I_j - R_j \tag{17}$$

for all $j \in \{1, \dots, M\}$. The unprocessed and processed data for France and Iran are depicted in Figure 2.

4.2 Parameter Identification

We only briefly sketch the parameter identification problem because it is an inverse problem [36, 37]. A deep discussion is out of the scope of this paper and would be a topic of own interest. We parameterize our time-varying transmission rates by $\alpha(t) = \alpha_1 \cdot \exp(-\alpha_2 \cdot t)$.

Applying a simple Nelder-Mead algorithm [38], we minimize the cost function

$$\begin{aligned}\mathcal{L}(\alpha_1, \alpha_2, \beta) = \sum_{j=1}^{M} \Bigg\{ & \left| S_{j+1} - S_j + \alpha_1 \cdot \exp(-\alpha_2 \cdot t_{j+1}) \cdot \frac{I_{j+1} \cdot S_{j+1}}{N} \right|^p \\ & \left| I_{j+1} - I_j - \alpha_1 \cdot \exp(-\alpha_2 \cdot t_{j+1}) \cdot \frac{I_{j+1} \cdot S_{j+1}}{N} + \beta \cdot I_{j+1} \right|^p \\ & \left| R_{j+1} - R_j - \beta \cdot I_{j+1} \right|^p \Bigg\}\end{aligned} \tag{18}$$

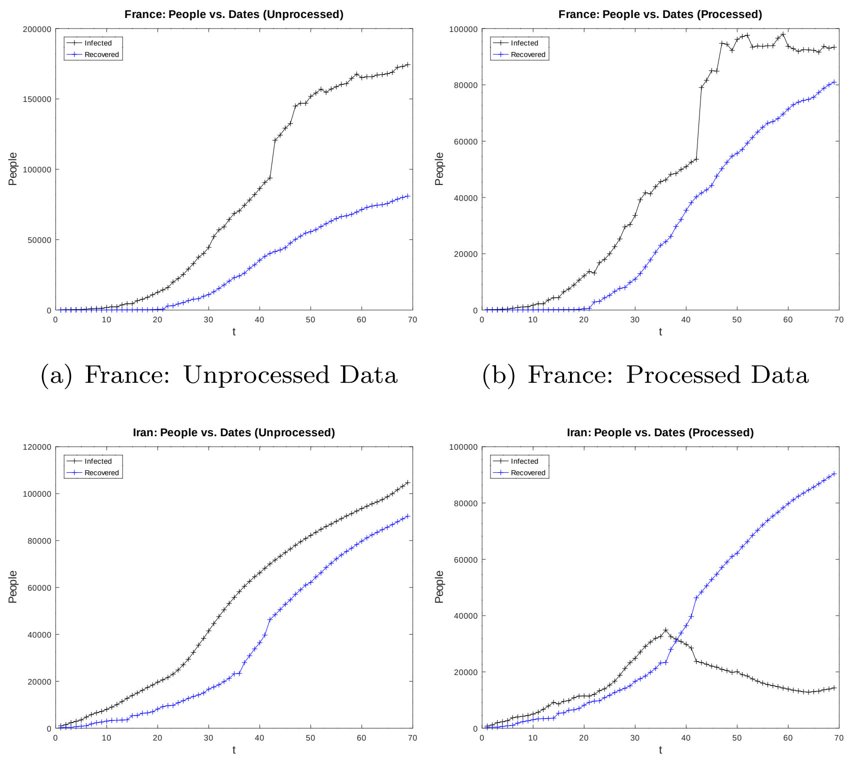

(a) France: Unprocessed Data (b) France: Processed Data

(c) Iran: Unprocessed Data (d) Iran: Processed Data

Figure 2 Unprocessed and processed data for France and Iran

for a user-chosen tuning parameter $p \in (0, \infty)$. The results for France and Iran are portrayed in Figure 3.

The calculated parameters can be picked from Table 2. Since our cost function (18), we go on without an error propagation analysis because our main scope is the detailed analysis of our numerical algorithm in Table 1.

Parameters	France	Iran
p	1.025	2.900
α_1	0.395	0.330
α_2	0.051	0.037
β	0.019	0.086

Table 2 Model parameters for $\alpha(t)$ and β

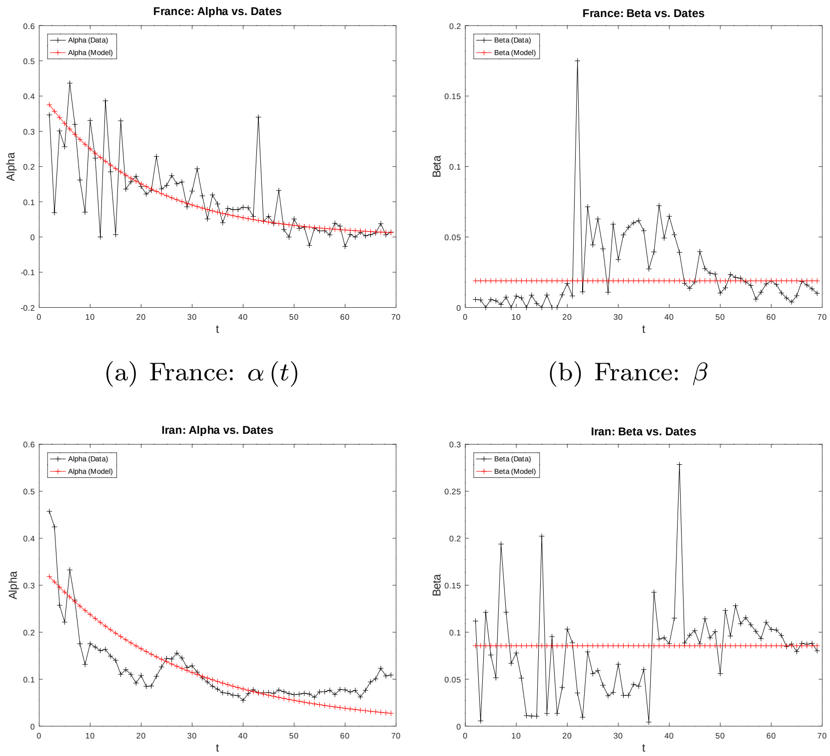

(a) France: $\alpha(t)$ (b) France: β

(c) Iran: $\alpha(t)$ (d) Iran: β

Figure 3 Model results for $\alpha(t)$ for France and Iran

Results can be also taken from our code which is available under `https://github.com/bewa87/2020-TimeDiscreteForwardSIR` like our used data from John Hopkins University [1, 2].

4.3 Results

The results of our forward algorithm from Table 1 for France and Iran can be seen in Figure 4.

5 Conclusion and Outlook

We established certain properties of the solution of our time-continuous SIR model in Section 2. Fortunately, we were able to transfer many continuous properties

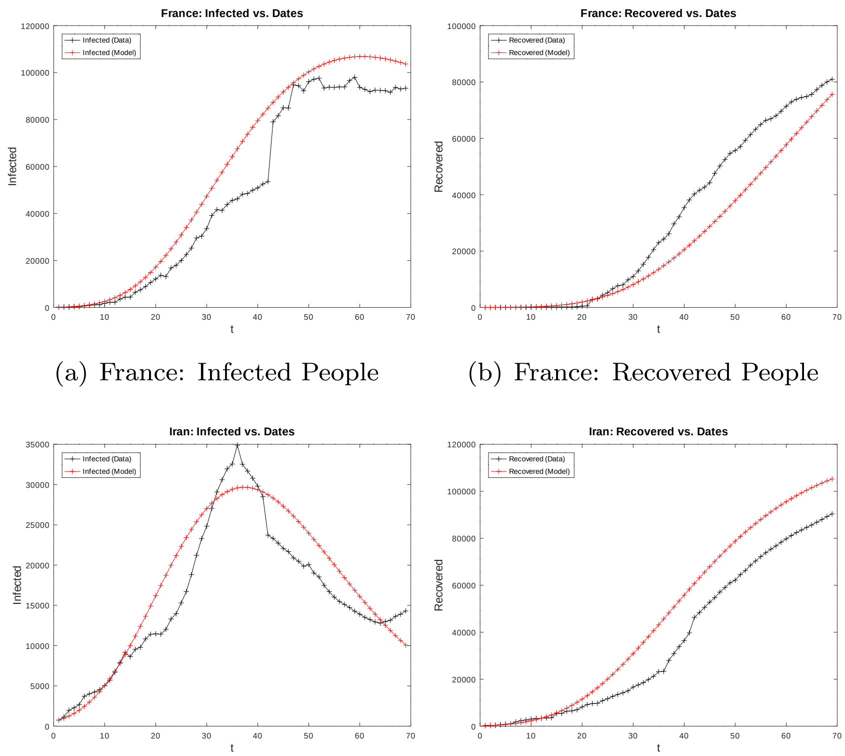

(a) France: Infected People (b) France: Recovered People

(c) Iran: Infected People (d) Iran: Recovered People

Figure 4 Forward model's forecasts for France and Iran

to our time-discrete implicit SIR model in Section 3 like unique solvability and monotonicity. In contrast to many other works mentioned in Section 1, we avoid an explicit forward model, but we could transform our implicit scheme to an explicit solution scheme. Thus, this makes our proposed scheme an attractive first prediction choice.

Regarding Figures 3 and 4, we see that our parametrization

$$\alpha\left(t\right)=\alpha_1\cdot\exp\left(-\alpha_2\cdot t\right)$$

is an appropriate fit for first forecasts considering the first wave of a spreading virus. Since these transmission rates are monotonically decreasing, we, however, remark that we will need to use another parametrization if we want to model diseases with seasonal behavior [39].

Additionally, we observe that our theoretical findings regarding monotonicity of recovered people from Theorem 6 is fulfilled in both examples.

As depicted in Section 4, the inverse problem definitely needs further investigation. This is a topic of its own interest. Furthermore, extension to further epidemiological forward models should be considered as we surely need more tools to predict the impact of upcoming epidemics.

Declarations

Availability of data and materials

Our code is freely available under `https://github.com/bewa87/2020-TimeDiscreteForwardSIR` as well as the data from France and Iran. Additional data are available under [2].

Competing interests

The authors declare that they have no competing interests.

Author's contributions

BW and JS designed the research. BW analyzed both models and implemented the time-discrete version. BW and JS analyzed data, discussed results and represented the data. BW and JS drafted and edited the manuscript.

Author details

[1]Next Generation Mobility Group, Max-Planck-Institute for Dynamics and Self-Organization, Department of Dynamics of Complex Fluids, Am Fassberg 17, D-37077 Göttingen, Germany. [2]Institute for Dynamics of Complex Fluids, Faculty of Physics, Georg-August-University of Göttingen, Friedrich-Hund-Platz 1, D-37077 Göttingen, Germany.

References

1. Dong, E, Du, H & Gardner, L: An Interactive Web-Based Dashboard to Track COVID-19 in Real Time. The Lancet - Infectious Diseases, `https://dx.doi.org/10.1016/S1473-3099(20)30120-1` (2020).
2. John Hopkins University (Dataset): Novel Coronavirus (COVID-19) Cases Data. `https://data.humdata.org/dataset/novel-coronavirus-2019-ncov-cases` (2020).
3. Zhou, P et al.: A Pneumonia Outbreak Associated with a New Coronavirus of Probable Bat Origin. Nature **579**:270–273, `https://dx.doi.org/10.1038/s41586-020-2012-7` (2020).
4. Chen, H et al.: Clinical Characteristics and Intrauterine Vertical Transmission Potential of COVID-19 Infection in Nine Pregnant Women: a Retrospective Review of Medical Records. The Lancet **395**(10226):809–815, `https://dx.doi.org/10.1016/S0140-6736(20)30360-3` (2020).

5. Xu, Z et al: Pathological Findings of COVID-19 Associated with Acute Respiratory Distress Syndrome. The Lancet - Respiratory Medicine **8**(4):420–422, https://dx.doi.org/10.1016/S2213-2600(20)30076-X (2020).
6. Wang, H & Zhang, L: Risk of COVID-19 for Patients with Cancer. The Lancet - Oncology **21**(4):E181, https://doi.org/10.1016/S1470-2045(20)30149-2 (2020).
7. Liu, Y et al: Aerodynamic Analysis of SARS-CoV-2 in Two Wuhan Hospitals. Nature, https://dx.doi.org/10.1038/s41586-020-2271-3 (2020).
8. Poyiadji, N et al.: COVID-19-Associated Acute Hemorrhagic Necrotizing Encephalopathy: CT and MRI Features. Radiology, https://dx.doi.org/10.1148/radiol.2020201187 (2020).
9. Grillet, F et al.: Acute Pulmonary Embolism Associated with COVID-19 Pneumonia Detected by Pulmonary CT Angiography. Radiology, https://dx.doi.org/10.1148/radiol.2020201544 (2020).
10. Kermack, W & McKendrick, A: A Contribution to the Mathematical Theory of Epidemics. Proceedings of the Royal Society London A **115**:700–721 (1927).
11. Kermack, W & McKendrick, A: Contributions to the Mathematical Theory of Epidemics - I. Bulletin of Mathematical Biology **53**(1-2):33-55, https://dx.doi.org/10.1007/BF02464423 (1991).
12. Kermack, W & McKendrick, A: Contributions to the Mathematical Theory of Epidemics - II. The Problem of Endemicity. Bulletin of Mathematical Biology **53**(1-2):57–87, https://dx.doi.org/10.1007/BF02464424 (1991).
13. Kermack, W & McKendrick, A: Contributions to the Mathematical Theory of Epidemics - III. Further Studies of the Problem of Endemicity. Bulletin of Mathematical Biology **53**(1-2):89–118, https://dx.doi.org/BF02464425 (1991).
14. Hethcote, HH: The Mathematics of Infectious Diseases. SIAM Review **42**(4):599–653, https://dx.doi.org/10.1137/S0036144500371907 (2000).
15. Murray, J.D.: Mathematical Biology II: Spatial Models and Medical Applications. In: Interdisciplinary Applied Mathematics, Vol. **18**, https://dx.doi.org/10.1007/b98869 (Springer, New York, 2003).
16. Brauer, F & Castillo-Chavez, C: Mathematical Models in Population Biology and Epidemiology. Springer, New York (2012).
17. Martcheva, M: An Introduction to Mathematical Epidemiology. Springer, New York (2015).
18. Iannelli, M & Milner, F: The Basic Approach to Age-Structured Population Dynamics: Models, Methods and Numerics. Springer, New York (2017).
19. Dehning, J et al.: Inferring COVID-19 Spreading Rates and Potential Change Points for Number Forecasts. https://arxiv.org/abs/2004.01105 (2020).
20. Fanelli, D & Piazza, F: Analysis and Forecast of COVID-19 Spreading in China, Italy and France. Chaos, Solitons & Fractals, https://dx.doi.org/10.1016/j.chaos.2020.109761 (2020).
21. He, S, Tang, S & Rong, L: A Discrete Stochastic Model of the COVID-19 Outbreak: Forecast and Control. Mathematical Biosciences and Engineering **17**(4):2792–2804, https://dx.doi.org/10.3934/mbe.2020153 (2020).
22. Flaxman, S et al.: Report 13: Estimating the Number of Infections and the Impact of Non-Pharmaceutical Interventions on COVID-19 in 11 European Countries. https://www.imperial.ac.uk/media/imperial-college/medicine/mrc-gida/2020-03-30-COVID19-Report-13.pdf (2020).
23. Flaxman, S et al.: Estimating the Number of Infections and the Impact of Non-Pharmaceutical Interventions on COVID-19 in European Countries: Technical Description Update. https://arxiv.org/abs/2004.11342 (2020).
24. Maier, BF & Brockmann, D: Effective Containment Explains Sub-Exponential Growth in Confirmed Cases of

Recent COVID-19 Outbreak in Mainland China. Science, https://dx.doi.org/10.1126/science.abb4557 (2020).

25. Gray, A et al.: A Stochastic Differential Equation SIS Epidemic Model. SIAM Journal of Applied Mathematics **71**(3):876–902, https://dx.doi.org/10.1137/10081856X (2011).
26. Osthus, D et al.: Forecasting Seasonal Influenza with a State-Space SIR Model. Annals of Applied Statistics **11**(1):202–224, https://dx.doi.org/10.1214/16-AOAS1000 (2017).
27. Al-Qaness, MAA, Ewees, AA, Fan, H & Abd El Aziz, M: Optimization Method for Forecasting Confirmed Cases of COVID-19 in China. Journal of Clinical Medicine **9**(3):674, https://dx.doi.org/10.3390/jcm9030674 (2020).
28. Brauer, F: The Kermack-McKendrick Epidemical Model Revisited. Mathematical Biosciences **198**(2):119–131, https://dx.doi.org/10.1016/j.mbs.2005.07.006 (2005).
29. Brauer, F: Some Simple Epidemic Models. Mathematical Biosciences and Engineering **3**(1):1–15, https://dx.doi.org/10.3934/mbe.2006.3.1 (2006).
30. Allen, LJS: Some Time-Discrete SI, SIR and SIS Epidemic Models. Mathematical Biosciences **124**(1):83–105, https://dx.doi.org/10.1016/0025-5564(94)90025-6 (1994).
31. Ma, X, Zhou, Y & Cao, H: Global Stability of the Endemic Equilibrium of a Discrete SIR Epidemic Model. Advances in Difference Equations **2013**:42, https://dx.doi.org/10.1186/1687-1847-2013-42 (2013).
32. De La Sen, M & Alonso-Quesada, S: Some Equilibrium, Stability, Instability and Oscillatory Results for an Extended Discrete Epidemic Model with Evolution Memory. Advances in Difference Equations **2013**:234, https://dx.doi.org/10.1186/1687-1847-2013-234 (2013).
33. Cantó, B, Coll, C & Sánchez, E: Estimation of Parameters in a Structured SIR Model. Advances in Differences Equations **2017**:33, https://dx.doi.org/10.1186/s13662-017-1078-5 (2017).
34. Schaeffer, DG & Cain, JW: Ordinary Differential Equations: Basics and Beyond. Springer, New York (2016).
35. Harko, T, Lobo, FSN & Mak, MK: Exact Analytics Solutions of the Susceptible-Infected-Recovered (SIR) Epidemic Model and of the SIR Model with Equal Death and Birth Rates. https://arxiv.org/pdf/1403.2160.pdf, (2014).
36. Tarantola, A: Inverse Problem Theory and Methods for Parameter Estimation. In: Other Titles in Applied Mathematics, Vol. **89**, https://dx.doi.org/10.1137/1.9780898717921. SIAM, Philadelphia (2005).
37. Marinov, TT, Marinova, RS, Omojola, J & Jackson, M: Inverse Problem for Coefficient Identification in SIR Epidemic Models. Computers & Mathematics with Applications **67**(12):2218–2227, https://dx.doi.org/10.1016/j.camwa.2014.02.002 (2014).
38. Nelder, JA & Mead, R: A Simplex Method for Function Minimization. The Computer Journal **7**(4):308–313, https://dx.doi.org/10.1093/comjnl/7.4.308 (1965).
39. Schanzer, DL, Sevenhuysen, C, Winchester, B & Mersereau, T: Estimating Influence Deaths in Canada, 1992-2009. PLoS One **8**(11):e80481, https://dx.doi.org/10.1371/journal.pone.0080481 (2013).